Available online at www.sciencedirect.com
SCIENCE DIRECT®
Pergamon
Cement and Concrete Research 34 (2004) 1057–1063
CEMENT AND CONCRETE RESEARCH

PhreeqC modeling of Friedel's salt equilibria at 23±1 °C

James V. Bothe Jr.*, Paul W. Brown

Department of Materials Science and Engineering, Pennsylvania State University, Materials Research Building, University Park, PA 16802, USA

Received 21 April 2003; accepted 21 November 2003

Abstract

A series of slurries containing Friedel's salt ($3CaO{\cdot}Al_2O_3{\cdot}CaCl_2{\cdot}10H_2O$) in equilibrium with other solids that include $Al(OH)_3$, $Ca(OH)_2$, and $3CaO{\cdot}Al_2O_3{\cdot}6H_2O$ were produced at room temperature (23 ± 1 °C). The liquid phases were analyzed for calcium, aluminum, and chlorine, and the speciation program PhreeqC was used to model the equilibria that were established between the solid and liquid phases. By matching closely, the experimentally determined solution parameters with those calculated using PhreeqC, important information concerning equilibria in the $CaO\text{-}Al_2O_3\text{-}CaCl_2\text{-}H_2O$ system was obtained. For example, it was shown that the stable phase pair, Friedel's salt/$3CaO{\cdot}Al_2O_3{\cdot}6H_2O$, acts to buffer against rising chloride concentrations by acting as a chloride sink. PhreeqC calculations have estimated the solubility product of Friedel's salt to fall within the range $-28.8 < \log K_{sp} < -27.6$.

Keywords: Friedel's salt; Speciation modeling; Phase equilibria

1. Introduction

Friedel's salt is a chloride-containing calcium aluminate hydrate found to exist as a stable hydration product in cement. It has the composition $3CaO{\cdot}Al_2O_3{\cdot}CaCl_2{\cdot}10H_2O$. There is an interest in Friedel's salt due to its role as a diffusion barrier against chloride ion, which causes corrosion of steel that is embedded in concrete [1–5]. Friedel's salt stability is of importance if concrete is to be used as a sealing material for a bedded salt repository that contains high-level radioactive waste [6]. Such an environment would expose the concrete to high concentrations of chloride. When $CaCl_2$ is used as an additive to concrete, the attendant formation of Friedel's salt plays an important role in the related cement chemistry [7,8].

Friedel's salt belongs to a family of compounds generally known as calcium aluminate or ferrite monosubstituted hydrates (AFm) phases, which are formed during cement hydration. Their crystal chemistry has been well documented; the structure comprises layers of calcium and aluminum, such as $[Ca_2Al(OH)_6]^+$, with water molecules and charge-compensating anions residing within the interlayer spaces [9–12]. These compounds tend to crystallize as platy hexagonal shaped crystals.

Phase equilibria studies play an important role in predicting the stability of various cement hydrates. Such information allows deterioration or strength-gain mechanisms to be determined. Landmark studies in this area have included the study of the system $CaO\text{-}Al_2O_3\text{-}CaSO_4\text{-}H_2O$ from which important hydrates such as ettringite and monosulfate precipitate [13,14]. In regards to Friedel's salt stability, while there have been prior studies on the system $CaO\text{-}Al_2O_3\text{-}CaCl_2\text{-}H_2O$ [5,6], these have not fully resolved the stabilities of the phases in this system.

In the present study, the system $CaO\text{-}Al_2O_3\text{-}CaCl_2\text{-}H_2O$ was further investigated by using the geochemical speciation program PhreeqC as a tool to quickly resolve effects of compositional changes on phase equilibria. By matching calculated with experimental data, PhreeqC was also used to derive a reasonable estimate for the solubility product of Friedel's salt.

2. Experimental methods

A series of slurries were made and analyzed to isolate various compositional points of interest within the $CaO\text{-}Al_2O_3\text{-}CaCl_2\text{-}H_2O$ system. Calcium chloride (Sigma; 99%

* Corresponding author. Tel.: +1-814-865-9291; fax: +1-814-863-7040.
E-mail address: jvb8@psu.edu (J.V. Bothe).

0008-8846/$ – see front matter © 2004 Elsevier Ltd. All rights reserved.
doi:10.1016/j.cemconres.2003.11.016

$CaCl_2 \cdot 2H_2O$) together with C_3A[1], CH, gibbsite (AH_3), and deionized water were mixed to form the desired phase assemblage. However, 25 wt.% excess $CaCl_2 \cdot 2H_2O$ was used to take into account its tendency to hydrate. The resulting slurries were contained in 125 ml high-density polyethylene bottles that were sealed tightly with their necks secured with electrical tape to minimize carbonation. The following are the phase assemblages that were made:

Bottle No.	Phase assemblage
1	Cl-AFm/C_3AH_6
2	Cl-AFm/CH
3	Cl-AFm/AH_3
4	Cl-AFm/C_3AH_6/CH
5	Cl-AFm/C_3AH_6/AH_3
6	Cl-AFm

Each phase assemblage was made by first hydrating C_3A in the presence of $CaCl_2 \cdot 2H_2O$ to form Cl-AFm (Friedel's salt). This was achieved by placing the mixture in a sealed polyethylene bottle, which also contained five pieces of zirconia-milling media on a roller mill overnight. The conditions associated with roller milling resulted in a temperature rise to around 45 °C. At this temperature, in conjunction with the continuous agitation, the reaction was accelerated resulting in highly crystalline X-ray pure Friedel's salt within 12 h. These conditions do not favor the formation of metastable hexagonal calcium aluminate hydrates. Once made, other ingredients were added to complete the phase assemblages desired. For example, additional C_3A was added to Bottle 1 to obtain Cl-AFm/C_3AH_6; portlandite, $Ca(OH)_2$, was added to Bottle 2 until Cl-AFm/CH was obtained; and gibbsite (Alcoa Hydral 710) was added to Bottle 3 until the phase assemblage Cl-AFm/AH_3 was achieved, and so on. Once the additional ingredients were added, the slurries were again placed onto the roller mill for another 12 h of mixing, then stored at room temperature (23 ± 1 °C), and periodically shaken over the course of approximately 6 months.

After 2 months from the time the mixtures were first made, a small sample of the solid phase was extracted from each bottle and analyzed. It was discovered that those samples that were anticipated to contain C_3AH_6 and CH as stable phases did not. For example, the C_3AH_6 in Bottle 1, 4, and 5 completely reacted. Therefore, additional C_3A was added to these slurries, which were then left to react for an additional 2 months. Upon analysis of the solid phases for a second time, it was discovered that C_3AH_6 was depleted in Bottle 1. After further C_3A addition, two additional months were allowed for the slurries to equilibrate, after which the desired phase assemblages were finally achieved. Fortification of the slurries was accompanied by another 12 h on the roller mill followed by equilibration at room temperature.

Table 1
Emission spectroscopy analysis of equilibrated solutions from the first set of samples

Sample No.	Al (mg/l)	Ca (mg/l)	Cl (mg/l)	Na (mg/l)
1	30	400	90	43
3	31	340	215	28
4	2.99	880	180	46
5	90	330	85	67
6	54	310	195	20

Once the reactions to produce the appropriate phase assemblages were complete and equilibrium reached, a portion of slurry was extracted from each bottle. The solution phases from the slurries were separated from the solids via centrifuging followed by filtration through a 0.2-μm syringe filter. Each solution phase was divided into two aliquots; a drop of 1 M HCl was added to one of these to preclude carbonate precipitation. The acidified solutions were later analyzed for calcium, sodium, and aluminum via emissions spectroscopy, whereas the other was analyzed for chlorine using ion chromatography. The results of these solution chemistry analyses are shown in Table 1.

The pH values were calculated for these slurries rather then directly measured because of rapid carbonation. Utilizing the concept of charge neutrality and the analytical values in Table 1, PhreeqC calculated the corresponding pH values for each sample. Concerning the measured sodium impurities, it was determined from a separate set of experiments that the source of the extraneous sodium ion came predominantly from the Bayer process alumina (gibbsite) and the C_3A, which was made from this aluminum source. Therefore, sodium was incorporated into the models as NaOH rather than NaCl.

3. Results

PhreeqC [15] modeling entails performing a series of mass-balance calculations to determine the lowest free energy configuration among the solid and solution phases. Input parameters are the number and identity of the solids present, their compositions, and the thermodynamic information related to their solubility in water. The solubility product of Cl-AFm is typically defined by the following dissociation equation:

$$\text{Cl-AFm} = 4Ca^{2+} + 2Al(OH)_4^- + 2Cl^- + 4OH^- : \log K_{sp} \quad (1)$$

[1] $C_3A = 3CaO \cdot Al_2O_3$; $C_3AH_6 = 3CaO \cdot Al_2O_3 \cdot 6H_2O$; $CH = CaO \cdot H_2O$; Cl-AFm = $C_3A \cdot CaCl_2 \cdot 10H_2O$.

Table 2
Equilibrium constants for those aqueous species and solid phases pertinent to the calculations performed by the computer program, PhreeqC

Species	Log K	Reference
Gibbsite, $Al(OH)_3$	7.75	[18]
Portlandite, $Ca(OH)_2$	22.80	[19]
C_3AH_6	81.10	[17, 20]
$Al(OH)_4^-$	22.80	[18]
$Ca(OH)^+$	12.68	[21]

However, PhreeqC treats Eq. (1) in terms of its primary components in the following manner:

$$\text{Cl-AFm} + 12H^+ = 4Ca^{2+} + 2Al^{3+} + 2Cl^- + 16H_2O : \log K_{rxn} \quad (2)$$

Eq. (2) was defined in the input file where the log K_{rxn} value can be changed after each simulation. Other solid and aqueous phases pertinent to the PhreeqC calculations have their thermodynamic information defined within the database (wateq4f.dat) [16], a separate file the program accesses, as well as listed in Table 2.

All PhreeqC calculations were performed at 25 °C due to limited thermodynamic information. However, the difference is less then 1% when comparing solubility products calculated at 22 and 25 °C of various calcium aluminates for which all the thermodynamic data are known [17].

3.1. Cl-AFm

Solution chemistry data obtained from Bottle 1 through 6 are presented in Table 1. The corresponding solid phase extracted from Bottle 6 was shown by X-ray diffraction (XRD) to be phase-pure Cl-AFm (Fig. 1). A speciation analysis by PhreeqC on the solution chemistry data from Bottle 6 converted molar concentrations of the components to their corresponding activities. These in turn were inserted into the expression for the solubility product of Cl-AFm:

$$K_{sp} = (Ca^{2+})^4(Al(OH)_4^-)^2(Cl^-)^2(OH^-)^4 \quad (3)$$

where the parentheses denote activity.

Table 3
Composition of solution in equilibrium with Cl-AFm

	Estimated log K	Al (mmol/l)	Ca (mmol/l)	Cl (mmol/l)	Na[a] (mmol/l)	pH
Analytical		2.00	7.73	5.50	0.87	11.85[b]
Simulation 1	72	2.93	5.86	2.93	0.87	11.74
Simulation 2	73	3.70	7.40	3.70	0.87	11.82
Simulation 3	74	4.67	9.35	4.67	0.87	11.90
Simulation 4	73.2	3.87	7.75	3.87	0.87	11.84
Simulation 5 ($CaCl_2$ = 0.75 mmol)	73.2	3.51	7.78	5.01	0.87	11.80

The corresponding XRD pattern is shown in Fig. 1.
[a] Na^+ incorporated into the model as NaOH.
[b] Calculated.

From Eq. (3), an initial estimate of log K_{sp} is −28.36, which when converted to conform to the reaction in Eq. (2) becomes 73.44 (log K_{rxn}). As a starting point, an estimate of 72 for Cl-AFm solubility was used and the input file adjusted to equilibrate solid Cl-AFm with the solution phase. The simulation was run again and the output data were compared with the solution chemistry data for single phase Cl-AFm. The simulation was repeated at least twice more using log K_{rxn} values of 73 and 74 in order to "book end" the best match between calculated and experimental values for the equilibrium concentrations of Al, Ca, and Cl, as well as for pH. Subsequent simulations were performed either to refine the estimated K_{rxn} value or to evaluate the effects of certain changes to the equilibria. These include adding excess $CaCl_2$, CO_2 (g), or allowing for the precipitation of gibbsite, which will be discussed in a later section. The results are presented in Table 3.

As shown in Table 3, increasing Cl-AFm solubility by increasing log K_{rxn} from 72 to 74 causes [Al] to diverge away from its analytical value while the remaining parameters converge toward their respective analytical values. However, [Cl] was consistently below its analytical value of 5.50 mmol/l. By running the simulation with excess $CaCl_2$, the match between the calculated and analytical [Cl] values was improved without significantly changing the other components. This assumption is reasonable

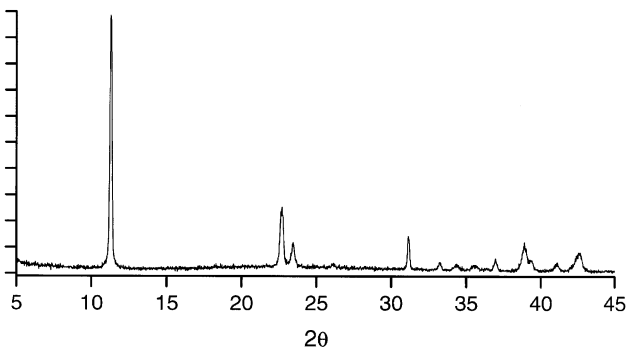

Fig. 1. XRD pattern of Friedel's salt (Sample 6).

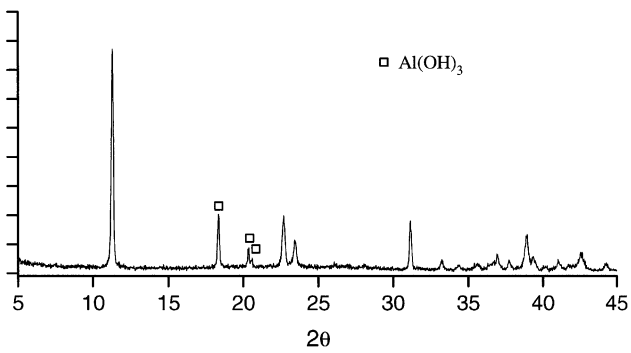

Fig. 2. XRD pattern of the Cl-AFm/AH_3 phase assemblage (Sample 3).

Table 4
Composition of solution in equilibrium with Cl-AFm and $Al(OH)_3$

	Estimated log K	Al (mmol/l)	Ca (mmol/l)	Cl (mmol/l)	Na (mmol/l)	pH
Analytical		1.15	8.48	6.06	1.22	11.94[a]
Simulation 1	72	1.12	6.54	3.27	1.22	11.91
Simulation 2	73	1.38	8.30	4.15	1.22	11.99
Simulation 3	74	1.69	10.56	5.28	1.22	12.07
Simulation 4 ($CaCl_2$ = 1.25 mmol)	73	1.20	8.38	6.07	1.22	11.93

The corresponding XRD pattern is shown in Fig. 2.
[a] Calculated.

Table 5
Composition of solution in equilibrium with Cl-AFm and C_3AH_6

	Estimated log K	Al (mmol/l)	Ca (mmol/l)	Cl (mmol/l)	Na (mmol/l)	pH
Analytical		1.11	9.98	2.54	1.87	12.15[a]
Simulation 1	72	4.71	7.34	0.53	1.87	11.96
Simulation 2	73	4.62	7.75	1.66	1.87	11.95
Simulation 3 ($CaCl_2$ = 1 mmol)	73	4.62	7.75	1.66	1.87	11.95
Simulation 4	74	4.37	9.03	4.96	1.87	11.92
Simulation 5 (gibbsite ↓)	73	1.86	9.13	1.60	1.87	12.12
Simulation 6 (gibbsite ↓)	73.5	1.82	9.59	2.79	1.87	12.11

The corresponding XRD pattern is shown in Fig. 3.
[a] Calculated.

considering excess $CaCl_2 \cdot 2H_2O$ was used in the preparations of the actual mixtures.

3.2. Cl-AFm/AH_3

Fig. 2 shows the diffraction pattern of the solids extracted from Bottle 3 and confirms the existence of the phase assemblage Cl-AFm/AH_3. The results of the analysis using PhreeqC are shown in Table 4. As with the previous analysis of single-phase Cl-AFm, the presence of excess $CaCl_2$ was again considered in the PhreeqC calculations to compensate for the high [Cl] determined experimentally. It can be seen from Table 4 that excess $CaCl_2$ further improved the match between the calculated and experimental data.

3.3. Cl-AFm/C_3AH_6

Fig. 3 shows the diffraction pattern of the solids extracted from Bottle 1. Table 5 presents the results of simulating this phase assemblage. By increasing log K_{rxn} to 74, the calculated [Cl] increases rather steeply and has quickly moved out of range. The model has also overestimated [Al]. Interestingly, the output data indicate the saturation index for gibbsite to be +0.57, which indicates the solution to be slightly supersaturated with respect to gibbsite. Allowing the gibbsite to precipitate and further refining the log K_{rxn} value resulted in a better match. Though gibbsite was not detected by XRD, it is possible that it may exist in amounts below the detection limit. This point will be further elaborated in the Discussion section.

The model also shows that adding a relatively small amount of $CaCl_2$ to the equilibria calculations has no effect on the properties of the solution phase. Inspection of the output data indicates that the C_3AH_6 acts to buffer additional chloride by producing more Cl-AFm.

3.4. Cl-AFm/C_3AH_6/AH_3

Bottle 5 represents one of two invariant compositions. Fig. 4 shows the diffraction pattern of the solids and confirms the appropriate phase assemblage. The analytical values of [Al] are modestly higher then those predicted by the model and the pH lower, as shown in Table 6. By using the values for [Ca] and [Cl] as benchmarks, a best match was obtained with a log K_{rxn} value between 73 and 74. As with the previous phase assemblage, the model predicted no change of the solution properties when exposed to excess $CaCl_2$.

Predictably, the optimum calculated values for the solution properties shown in Table 6 are similar to those presented in Table 5 for Cl-AFm/C_3AH_6. Yet, the analytical values do not suggest these two phase assemblages be representative of the same invariant point. The reason for

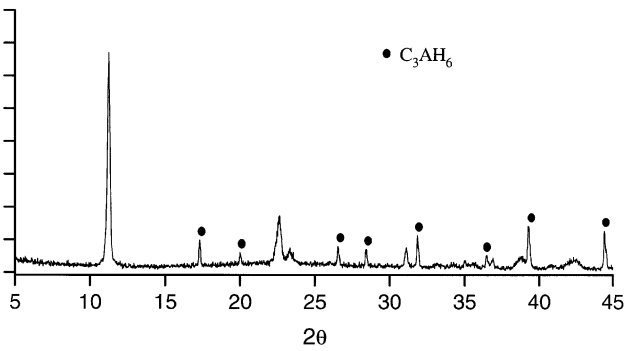

Fig. 3. XRD pattern of the Cl-AFm/C_3AH_6 phase assemblage (Sample 1).

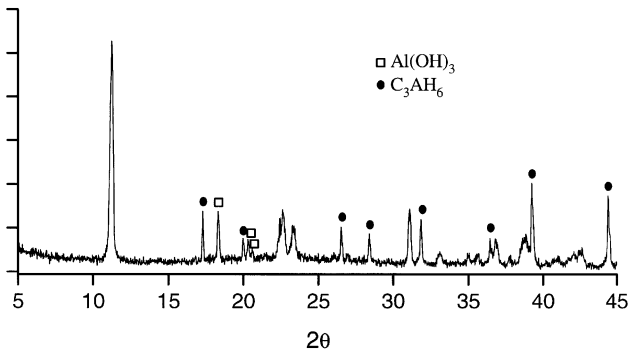

Fig. 4. XRD pattern of invariant phase assemblage Cl-AFm/C_3AH_6/AH_3 (Sample 5).

Table 6
Composition of solution in equilibrium with Cl-AFm, C_3AH_6, and $Al(OH)_3$

	Estimated log K	Al (mmol/l)	Ca (mmol/l)	Cl (mmol/l)	Na (mmol/l)	pH
Analytical		3.34	8.23	2.40	2.91	12.03[a]
Simulation 1	72	1.93	8.39	0.52	2.91	12.14
Simulation 2	73	1.90	8.80	1.63	2.91	12.13
Simulation 3 ($CaCl_2$ = 1 mmol)	73	1.90	8.80	1.63	2.91	12.13
Simulation 4	74	1.80	10.05	4.91	2.91	12.10
Simulation 5	73.25	1.88	8.99	2.16	2.91	12.12
Simulation 6 Log K (gibbsite) = 8.11	73.5	3.34	8.18	2.93	2.91	12.01

The corresponding XRD pattern is shown in Fig. 4.
[a] Calculated.

Table 7
Composition of solution in equilibrium with Cl-AFm, C_3AH_6, and $Ca(OH)_2$

	Estimated log K	Al (mmol/l)	Ca (mmol/l)	Cl (mmol/l)	Na (mmol/l)	pH
Analytical		0.11	21.96	5.08	2.00	12.46[a]
Simulation 1	72	0.18	20.33	0.42	2.00	12.48
Simulation 2	73	0.18	20.68	1.31	2.00	12.48
Simulation 3	74	0.17	21.79	4.07	2.00	12.46
Simulation 5	74.20	0.17	22.20	5.08	2.00	12.46
Simulation 6 [CO_2(g) = 1 mmol, calcite ↓]	74.20	0.17	22.20	5.08	2.00	12.46

The corresponding XRD pattern is shown in Fig. 5.
[a] Calculated.

the higher [Al] is uncertain and it is doubtful that the gibbsite would behave any differently in this phase assemblage than it would in the assemblage Cl-AFm/AH_3 (compare Figs. 2 and 4). Hypothetically, increasing the solubility of gibbsite to make the calculated and experimental values of [Al] match would still produce an optimal log K_{rxn} value between 73 and 74, as shown in Table 6.

3.5. Cl-AFm/C_3AH_6/CH

XRD confirms the invariant phase assemblage but indicates the presence of a small amount of calcite, $CaCO_3$, as shown in Fig. 5. It is not certain whether the calcite formed upon drying or was formed during equilibration. Regardless, the presence of $CaCO_3$ has a negligible effect on the solution properties as long as solid $Ca(OH)_2$ is present as a stable equilibrium phase. The PhreeqC simulations modeled fairly accurately this equilibrium phase assemblage, as shown in Table 7. When exposed to 1 mmol of CO_2 (g), the model predicted the solution to become supersaturated with respect to calcite. When allowed to precipitate, the calcite had no effect on the calculated properties of the solution phase. The model showed that only a small amount of solid $Ca(OH)_2$ was consumed instead.

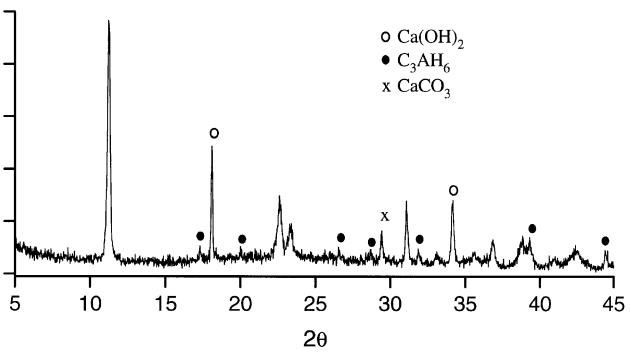

Fig. 5. XRD pattern of the invariant phase assemblage Cl-AFm/C_3AH_6/CH (Sample 4).

4. Discussion

Sodium was found to be present in all mixtures made during this study and as mentioned previously came predominantly from the aluminum-containing ingredients. The Cl-AFm/C_3AH_6/AH_3 phase assemblage contained the most sodium, which was determined to be 2.91 mmol/l. This is consistent with this phase assemblage being the most abundant in aluminum. By removing the Na from all calculations, PhreeqC determined its effects on solution chemistry to be minimal. The changes in pH, [Al], [Ca], and [Cl] were all under 6%, which is within experimental error (~ 10%) associated with measuring these parameters.

PhreeqC modeling of the Cl-AFm/C_3AH_6 phase assemblage predicts the equilibrium [Al] to be relatively high and the solution to be supersaturated with respect to gibbsite. This is not unreasonable given the starting materials used. According to prior studies [22–24], C_3A dissociates incongruently releasing calcium into solution to a greater extent, thereby forming an aluminum-rich layer on the surface of the C_3A particle. This layer may persist metastably as an amorphous hydrogel [13]. Over time, these metastable forms will tend to convert to crystalline gibbsite.

As the simulations in Tables 5 and 6 show, the phase assemblages containing the hydrogarnet (C_3AH_6)/Cl-AFm combination demonstrated a capacity for buffering chloride ion. According to the PhreeqC model, this is accomplished through the consumption of C_3AH_6 and the simultaneous production of Cl-AFm. To demonstrate this behavior, multiple equilibria simulations of the phase assemblage Cl-AFm/C_3AH_6/AH_3 were performed while increasing the amounts of chloride present. Using a log K_{rxn} value of 73.5 for Cl-AFm and starting with 0.01 moles each of Cl-AFm and C_3AH_6, the properties of the solution phase, along with the amounts of solid phases present, were plotted in Figs. 6 and 7 for NaCl and $CaCl_2$, respectively. As shown in the figures, the buffering capacity of this phase assemblage

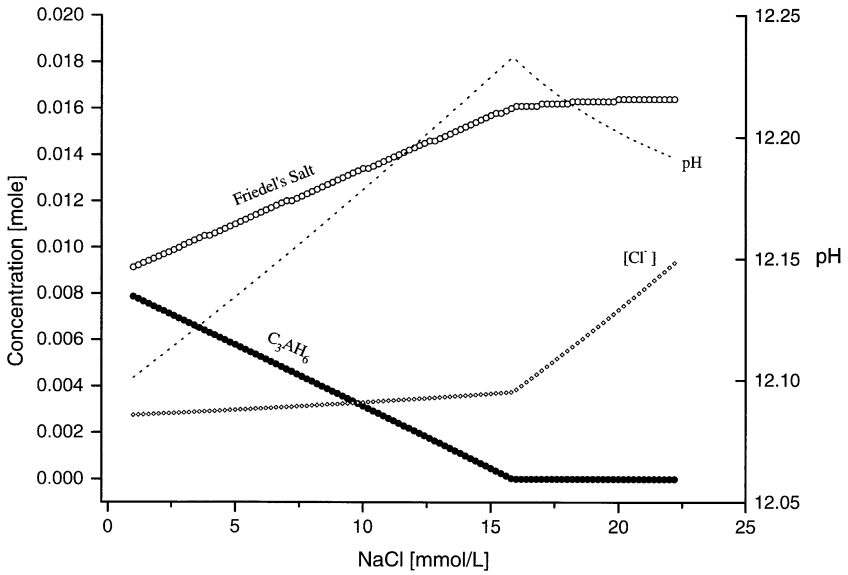

Fig. 6. Plot showing trends in solution chemistry of the AFm/C_3AH_6/AH_3 phase assemblage as a function of NaCl concentration.

is exhausted when C_3AH_6 is consumed. Beyond this point, the composition moves away from the invariant point and along the univariant phase boundary Cl-AFm/AH_3 toward higher chloride concentrations.

There are other interesting trends worth noting concerning these plots. For NaCl (Fig. 6), the pH rises steadily with added chloride. This is attributed to the reaction of chloride with C_3AH_6 to form Friedel's salt leaving Na^+ as NaOH. However, once the C_3AH_6 has been consumed, [Cl] will dominate the solution phase causing the equilibria to shift in favor of less hydroxyl in accordance with Eq. (3), thereby lowering the pH slightly. In contrast, when $CaCl_2$ is used (Fig. 7), the calculated pH remains constant as long as C_3AH_6 is present. When C_3AH_6 has disappeared, the calculated pH values drop precipitously with further $CaCl_2$ additions. This trend can be explained by Eq. (3) and the common ion effect. As [Ca] and [Cl] increases, equilibrium constraints will force [OH] to decrease.

When increasing amounts of NaCl are added to the invariant phase assemblage, the composition of the solution phase changes as calcium and aluminum are removed from solution to form more solid Cl-AFm. During these changes, the model predicts a decrease in $[Ca^{2+}]$ causing a slight rise in [Cl] (Fig. 6) due to the equilibrium constraints of Eq. (3). In contrast, the properties of the solution phase do not change when $CaCl_2$ is added to the invariant composition

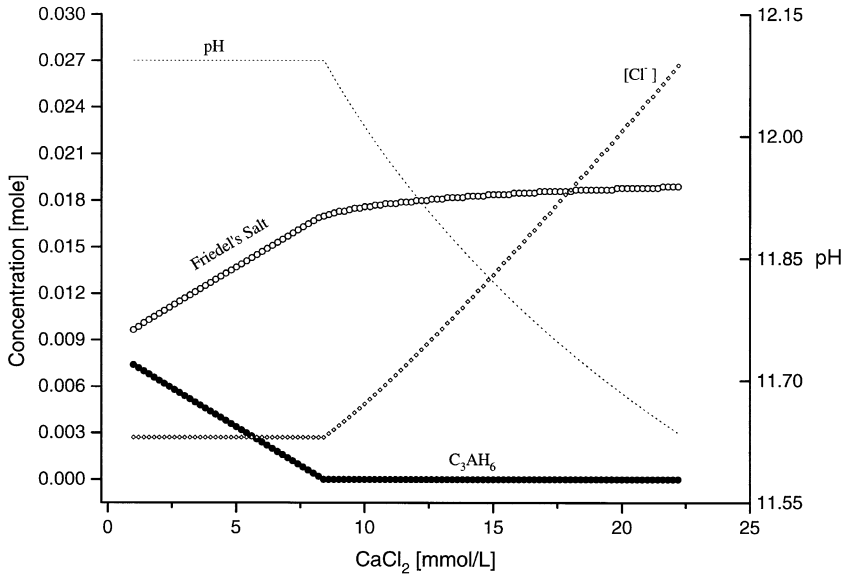

Fig. 7. Plot showing trends in solution chemistry of the AFm/C_3AH_6/AH_3 phase assemblage as a function of $CaCl_2$ concentration.

and [Cl] (Fig. 7) remains constant as long as C_3AH_6 is present. After the C_3AH_6 has been consumed, the amount of Cl-AFm continues to increase with increasing amounts of either NaCl or $CaCl_2$.

5. Conclusions

PhreeqC has been used to facilitate the discovery of trends within a specified compositional boundary related to aqueous-based phase equilibria. In the present study, PhreeqC modeling showed how Friedel's salt, when in the presence of C_3AH_6, acts to buffer excess chloride ion. Also, by matching the calculated solution parameters with those analytically measured, the log K_{rxn} was estimated to be between 73 and 74.2. These values translate to a solubility product for Friedel's salt estimated to be within the range $-28.8 < \log K_{sp} < -27.6$. Others published in the literature are -27.10 and -24.768 [5].

References

[1] M.A. Sanjuan, Formation of chloroaluminates in calcium aluminate cements cured at high temperatures and exposed to chloride solutions, J. Mater. Sci. 32 (1997) 6207–6213.

[2] Rasheeduzzafar, S.S. Al-Saadoun, A.S. Al-Gahtani, F.H. Dakhil, Effect of tricalcium aluminate content of cement on corrosion of reinforcing steel in concrete, Cem. Concr. Res. 20 (1990) 723–738.

[3] S. Goni, A. Guerrero, Accelerated carbonation of Friedel's salt in calcium aluminate cement paste, Cem. Concr. Res. 33 (2002) 21–26.

[4] A.K. Suryavanshi, J.D. Scantlebury, S.B. Lyon, Mechanism of Friedel's salt formation in cement rich in tri-calcium aluminate, Cem. Concr. Res. 26 (1996) 717–727.

[5] S.U.A. Birnin-Yauri, F.P. Glasser, Friedel's salt, $Ca_2Al(OH)_6(Cl,OH)\cdot 2H_2O$: Its solid solutions and their role in chloride binding, Cem. Concr. Res. 28 (1998) 1713–1723.

[6] C. Abate, B.E. Scheetz, Aqueous phase equilibria in the system $CaO-Al_2O_3-CaCl_2-H_2O$: The significance and stability of Friedel's salt, J. Am. Ceram. Soc. 78 (1995) 939–944.

[7] H.B. Lackey, Factors affecting use of calcium chloride in concrete, Cem., Concr. Aggreg. 14 (1992) 97–100.

[8] A. Traetteberg, P.E. Grattan-Bellew, Hydration of $3CaO\cdot Al_2O_3$ and $3CaO\cdot Al_2O_3$ + gypsum with and without $CaCl_2$, J. Am. Ceram. Soc. 58 (1975) 221–227.

[9] R. Fischer, H.J. Kuzel, Reinvestigation of the system $C_4A\cdot nH_2O$-$C_4A\cdot CO_2\cdot nH_2O$, Cem. Concr. Res. 12 (1982) 517–526.

[10] H.F.W. Taylor, Crystal structures of some double hydroxide minerals, Min. Mag. 39 (1973) 377–389.

[11] H.J. Kuzel, X-ray investigation of some complex calcium aluminate hydrates and related compounds, 5th International Symposium on the Chemistry of Cements, II-9, Tokyo, 1968, pp. 92–97.

[12] S.J. Ahmed, H.F.W. Taylor, Crystal structures of the lamellar calcium aluminate hydrates, Nature 215 (1967) 622–623.

[13] F.E. Jones, The quaternary system $CaO-Al_2O_3-CaSO_4-H_2O$ at 25 °C, J. Phys. Chem. 48 (1944) 311–356.

[14] W. Eitel, Recent investigations of the system lime-alumina-calcium-sulfate-water and its importance in building research problems, J. Am. Concr. Inst. 28 (1957) 679–698.

[15] D.L. Parkhurst, C.A.J. Appelo, User's Guide to PhreeqC (Version 2)—A Computer Program for Speciation, Batch-Reaction, One-Dimensional Transport, and Inverse Geochemical Calculations, U.S. Geological Survey, Water-Resources Investigations Report 99-4259, Denver, CO, 1999.

[16] J.W. Ball, D.K. Nordstrom, WATEQ4F—Users Manual with Revised Thermodynamic Data Base and Test Cases for Calculating Speciation of Major, Trace and Redox Elements in Natural Waters, U.S. Geological Survey, Open-File Report 90-129, Denver, CO, 1991.

[17] J.V. Bothe Jr., P.W. Brown, Phase Equilibria in the System $CaO-Al_2O_3-B_2O_3-H_2O$ at 23 ± 1 °C, Adv. Cem. Res. 10 (1998) 121–127.

[18] D.J. Wesolowski, Aluminum speciation and equilibria in aqueous solution: I. The solubility of gibbsite in the system Na-K-Cl-OH-$Al(OH)_4$ from 0 to 100 °C, Geochim. Cosmochim. Acta 56 (1992) 1065–1091.

[19] J. Duchesne, E.J. Reardon, Measurement and prediction of portlandite solubility in alkali solutions, Cem. Concr. Res. 25 (1995) 1713–1723.

[20] V. Babushkin, Thermodynamics of Silicates, Springer-Verlag, Berlin, 1985.

[21] V. Wagman, et al., NBS tables of chemical thermodynamic, J. Phys. Chem. 11 (Suppl. 2) (ref. data).

[22] S. Chatterji, Mechanisms of retardation of C_3A: A critical evaluation, 7th International Congress on the Chemistry of Cement, IV, Paris, 1980, pp. 465–470.

[23] J. Skalny, M.E. Tadros, Retardation of tricalcium aluminate hydration by sulfates, J. Am. Ceram. Soc. 60 (1977) 174–175.

[24] P.W. Brown, The implications of phase equilibria on hydration in the tricalcium silicate-water and the tricalcium aluminate-gypsum-water systems, 8th International Symposium on the Chemistry of Cement, Vol. III, Rio, 1986, pp. 231–239.